2000

# The Extended and Eccentric E-DNA Structure Induced by Cytosine Methylation or Bromination

Jeff Vargason
*George Fox University*, jvargason@georgefox.edu

Brandt F. Eichman
*Oregon State University*

P. Shing Ho
*Oregon State University*, hops@ucs.orst.edu



Recommended Citation
Previously published in Nature Structural Biology, 2000, volume 7, pp. 758-761 http://www.nature.com/nsmb/journal/v7/n9/full/nsb0900_758.html

# The extended and eccentric E-DNA structure induced by cytosine methylation or bromination

Jeffrey M. Vargason, Brandt F. Eichman and P. Shing Ho

*Department of Biochemistry and Biophysics, ALS 2011, Oregon State University, Corvallis, Oregon 97331-7305, USA.*

**Cytosine methylation or bromination of the DNA sequence d(GGCGCC)$_2$ is shown here to induce a novel extended and eccentric double helix, which we call E-DNA. Like B-DNA, E-DNA has a long helical rise and bases perpendicular to the helix axis. However, the 3′-*endo* sugar conformation gives the characteristic deep major groove and shallow minor groove of A-DNA. Also, if allowed to crystallize for a period of time longer than that yielding E-DNA, the methylated sequence forms standard A-DNA, suggesting that E-DNA is a kinetically trapped intermediate in the transition to A-DNA. Thus, the structures presented here chart a crystallographic pathway from B-DNA to A-DNA through the E-DNA intermediate in a single sequence. The E-DNA surface is highly accessible to solvent, with waters in the major groove sitting on exposed faces of the stacked nucleotides. We suggest that the geometry of the waters and the stacked base pairs would promote the spontaneous deamination of 5-methylcytosine in the transition mutation of dm$^5$C-dG to dT-dA base pairs.**

5-Methyldeoxycytidine (dm$^5$C) is often considered the fifth nucleotide of the genetic code. Prokaryotes use cytosine methylation to distinguish parent from replicated daughter DNAs, and host from viral DNAs[1]. In eukaryotes, dm$^5$C has been implicated in processes as varied as X-chromosome inactivation, genomic imprinting, and gene inactivation[2–4]. The effect of cytosine methylation on double helical DNA, therefore, has been of great interest over the years. Cytosine methylation and bromination have been shown to stabilize A-DNA[5,6] and left handed Z-DNA[7,8]. However, neither A-DNA nor Z-DNA requires cytosine methylation for its formation; therefore, methylation serves to facilitate rather than induce these conformations. The question is whether methylation can induce a unique structure.

Here, we show that the sequence d(GGCGCC)$_2$ crystallizes as standard B-DNA, while the sequences d(GGCGm$^5$CC)$_2$ and d(GGCGBr$^5$CC)$_2$ form a new conformation, which we call E-DNA, that has structural characteristics of both B-DNA and A-DNA (Fig. 1*a*). The B-DNA and E-DNA sequences were crystallized under nearly identical conditions indicating that, unlike A-DNA[5], E-DNA does not require dehydration. Interestingly, the sequence d(GGCGm$^5$CC)$_2$ crystallizes as E-DNA over two to three weeks, but when allowed to crystallize for two to three months forms a standard A-DNA double helix. Finally, we suggest that E-DNA may play a role in the transition mutation of dm$^5$C-dG to dT-dA base pairs in the cell.

## B-DNA structure of d(GGCGCC)$_2$

The sequence d(GGCGCC)$_2$ was crystallized as B-DNA in the presence of spermine hydrochloride (spermine$^{4+}$) alone or with cobalt hexamine (Co(NH$_3$)$_6^{3+}$) (Fig. 2*a*). In both crystal forms, the DNA duplexes stack coaxially to form the continuous columns seen previously in B-DNA crystals[9]. The deoxyriboses in the four unique duplex structures determined here, three from the spermine$^{4+}$ form and one from the Co(NH$_3$)$_6^{3+}$ form, all fall into the family of 2′-*endo* conformations of B-DNA. The helical parame-

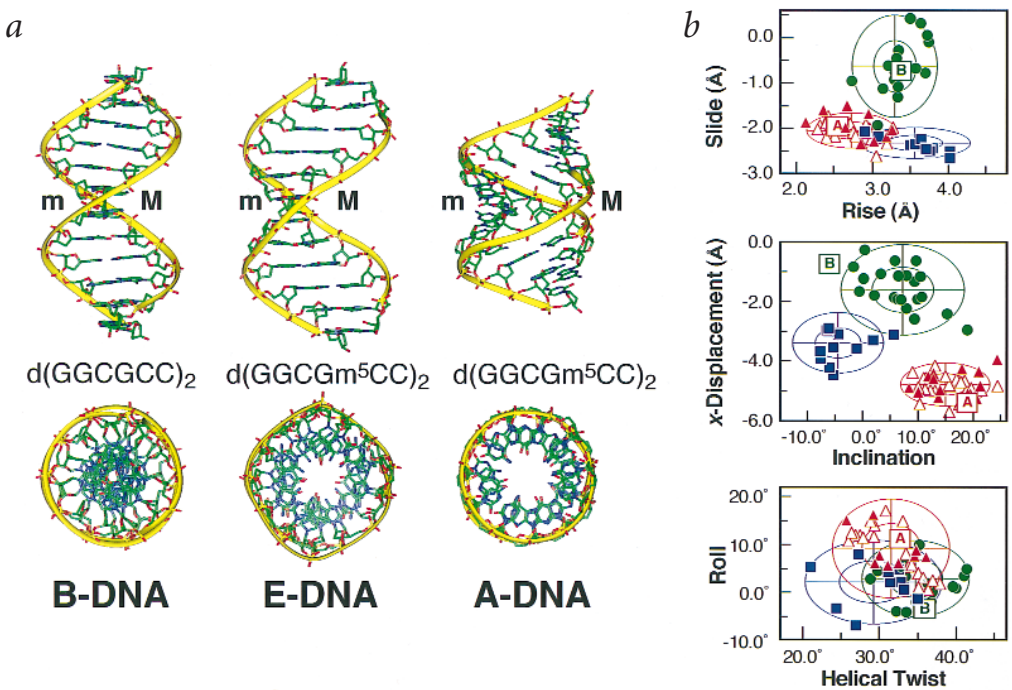


**Fig. 1** Comparing E-DNA with B-DNA and A-DNA. ***a***, Views into (top) and down (bottom) the helix axes of 12-base pair models constructed from the crystal structures of d(GGCGCC)$_2$ as B-DNA, and d(GGCGm$^5$CC)$_2$ as E-DNA and as A-DNA. The phosphodeoxyribose backbones are traced by yellow ribbons. ***b***, Helical parameters (calculated by CURVES 5.2; ref. 22) of hexanucleotide structures containing dC-dG, dm$^5$C-dG, and dBr$^5$C-dG base pairs as B-DNA (green circles), A-DNA (red triangles), and E-DNA (blue squares). Parameters determined from the current structures are shown as filled symbols, while those from the previously published A-DNA structures[5] are open. Concentric ovals represent 1 and 2 standard deviations from the mean. Parameters for A-DNA and B-DNA fibers are indicated by the boxed A and B, respectively.

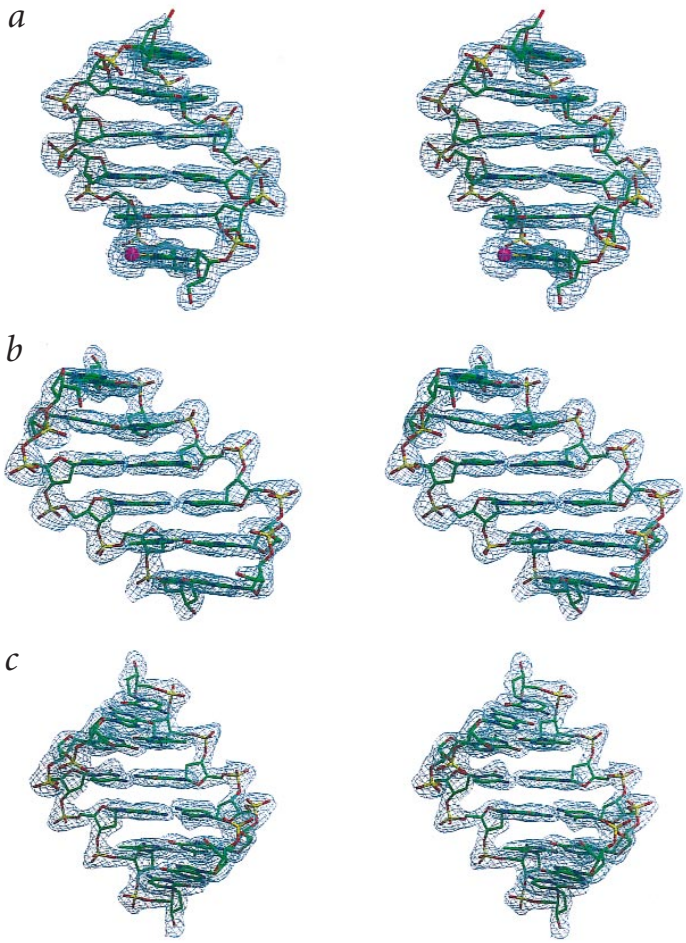


**Fig. 2** Electron density maps showing stereo views looking into the major grooves of the B-, E-, and A-DNA structures. ***a***, $d(GGCGCC)_2$ with $Co^{3+}$ (purple sphere) as B-DNA; ***b***, $d(GGCGm^5CC)_2$ as E-DNA; ***c***, $d(GGCGm^5CC)_2$ as A-DNA. The $2F_o - F_c$ maps are contoured at 1 σ. This figure was rendered with Raster3D[23].

ters (Fig. 1*b*) show sequence dependent variations that deviate from fiber B-DNA, but are all clearly standard B-DNA, even though $Co(NH_3)_6^{3+}$ has been shown to promote the formation of A-DNA in solution[10]. The polycations in the crystals act as the molecular glue that holds the lattices together. One spermine$^{4+}$ spans the major groove of two stacked duplexes, while a second bridges the backbones of two unstacked duplexes in the spermine$^{4+}$ form. In contrast, the cobalt metal in the $Co(NH_3)_6^{3+}$ form directly crosslinks the guanines of two symmetry related duplexes.

## E-DNA structure of $d(GGCGm^5CC)_2$ and $d(GGCGBr^5CC)_2$

The sequences $d(GGCGm^5CC)_2$ and $d(GGCGBr^5CC)_2$ were crystallized from solutions that were nearly identical to the spermine$^{4+}$ form of $d(GGCGCC)_2$. The crystal structures of $d(GGCGm^5CC)_2$ and $d(GGCGBr^5CC)_2$ are nearly identical, consisting of right handed antiparallel double helices (Fig. 2*b*). Viewed into the helix (Fig. 1*a*), the structures appear to be variants of B-DNA with base pairs lying perpendicular to, and extended along, the helix axis. However, we see the deep major groove and shallow minor groove that is associated with the 3′-*endo* deoxyribose sugar conformation of A-DNA. Looking down the helix, the backbone traces a squared rather than a circular cylinder. The structure, therefore, has features of both A-DNA and B-DNA; however, it is neither. This new structure is called 'E-DNA' to recognize the extended helix and the eccentric trace of the backbone.

A detailed analysis (Fig. 1*b*, Table 1) shows E-DNA to be distinct from A-DNA and B-DNA. The slight negative inclination of the base pairs is more like fiber B-DNA than even the B-DNA structures of $d(GGCGCC)_2$. However, like A-DNA, the large negative x-displacement places the helix axis in the major groove. The eccentric backbone results from an even greater protrusion of the modified cytosines away from the helix axis than in A-DNA, as is evident from the more negative x-displacement. In addition, the shortened distance between phosphates of the modified (5.7 ± 0.2 Å) *versus* unmodified base pairs (6.5 ± 0.3 Å) is comparable to differences between A-DNA (5.8 ± 0.2 Å) and B-DNA (6.6 ± 0.3 Å). The average rise is longer than that of B-DNA, and the average slide between base pairs is larger than in A-DNA. Thus, E-DNA is more extended and broader than A-DNA and B-DNA, and shows variations associated with the modifications to the cytosine bases.

The E-DNA crystal lattice has one terminal base pair of the duplex sitting in the minor groove of a symmetry related duplex, which is typical of A-DNA crystals[5]. The opposite end of the duplex, however, is coaxially stacked, similar to the $d(GGCGCC)_2$ crystals. Therefore, rather than the crystal interactions defining the conformation, it appears that E-DNA defines a conglomerate crystal lattice.

Interestingly, it is the B-DNA type stacking interactions that show the greatest lattice distortions to the E-DNA structure. The stacked base pairs at these termini are dramatically underwound, with an average helical twist of 23.7°. The average helical twist estimated from the remainder of the nucleotides is equivalent to a helical repeat of 11.8 base pairs per turn, making E-DNA an underwound structure relative to both A-DNA and B-DNA.

E-DNA is not a chimeric structure. *Cis*-platin, for example, sits at a junction between B-DNA and A-DNA[11], while DNA/RNA hybrids have distinct A-RNA and B-DNA strands[12]. These chimeric structures have the two conformations coexisting in the same molecule. A-DNA and B-DNA have also been shown to coexist as unique structures within a single crystal lattice[13], while the sequence $d(CCGCCGGCGG)_2$ has been crystallized as both A-DNA[14] and B-DNA[15]. E-DNA, however, has structural properties of both conformations, but cannot be readily classified as either a variation of B-DNA or of A-DNA, or as a chimera of the two. Finally, with its extended rise and large slide between base pairs, E-DNA distinguishes itself from the intermediate structures of $d(CCCCGGGG)_2$ (ref. 16) and $d(CATGGGCCCATG)_2$ (ref. 17), both of which fall within the continuum between B-DNA and A-DNA.

## A-DNA structure of $d(GGCGm^5CC)_2$

The sequence $d(GGCGm^5CC)_2$ crystallized as standard A-DNA from identical solutions that yielded E-DNA crystals of this same sequence. The difference was that the A-DNA crystals of this sequence (Fig. 2*c*) grew after a significantly longer period of time (two to three months compared to two to three weeks for the E-DNA crystals). The asymmetric unit of the crystals was composed of two complete A-DNA duplexes, and one duplex with one terminal base pair melted. We could not accurately account for this frayed end, and therefore, did not incorporate this model into our analysis of the structure. The conformation obtained from these 'aged' solutions had large positive inclination angles, negative x-displacements and negative slides, and short helical rises between base pairs (Fig. 1*b*). These helical parameters, along with

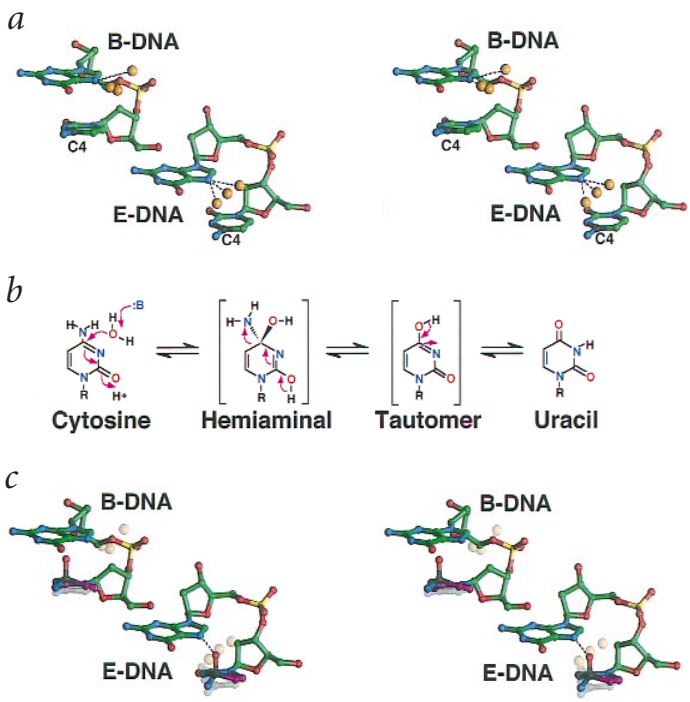


**Fig. 3** Waters in the CpG dinucleotides of B-DNA and E-DNA. ***a***, Stereo view of waters (gold spheres) hydrogen bonded (broken lines) to the guanine at the CpG steps in $d(GGCGCC)_2$ as B-DNA, and in $d(GGCGm^5CC)_2$ and $d(GGCGBr^5CC)_2$ as E-DNA. The waters are overlaid relative to the guanine N7 nitrogen of an average structure built from three unique CpG steps found in each conformation (the C4 carbon of the cytosine base is colored black). ***b***, Mechanism for the spontaneous deamination of cytosine to uracil[24]. The nucleophilic attack of a water molecule at the C4 carbon forms a hemiaminal intermediate. Release of ammonia results in a tautomer, which subsequently rearranges to uracil. ***c***, Model of the hemiaminal intermediate in B-DNA and E-DNA. The hemiaminal intermediate at the CpG step was modeled by adding a hydroxyl group to the C4 carbon (colored black) of the cytosine base, followed by geometry optimization using the AMBER[25] force field as implemented in the program InsightII (Biosym/MSI). The starting positions of the waters and the starting cytosine base are shown as transparent overlays.

the 3′-*endo* sugar conformations, are characteristic of A-DNA. Finally, the interduplex interactions were typical of hexanucleotide A-DNA crystals[5]. In short, there was nothing that set this crystal structure apart from other undistorted A-DNA structures.

## E-DNA intermediate in the B-DNA to A-DNA transition

One of the truly unique results from this study is that a single sequence, $d(GGCGCC)_2$, has been crystallized as standard B-DNA and A-DNA double helices, and also shown to form a novel structure, E-DNA, which is intermediate between the two. The requirement for methylation to induce A-DNA in this sequence is consistent with previous observations that $dm^5C$ nucleotides induce the transition from B-DNA to A-DNA[5,6]. The shorter period of time required to grow crystals of E-DNA from identical solutions that eventually yielded A-DNA indicates that this intermediate was kinetically trapped by crystallization. We show here that the methyl group facilitates the conversion of the sugar conformation from 2′-*endo* to 3′-*endo*, which is apparently the rate-limiting step for the B-DNA to A-DNA transition. Thus, the transition from B-DNA to A-DNA occurs through E-DNA as a discrete intermediate, and, at least for the methylation induced transition, this intermediate is elongated and underwound relative to either B-DNA or A-DNA. The structural convolutions that lead from B-DNA to E-DNA and finally to A-DNA are apparent from the views into the major grooves of the three crystal structures (Fig. 2). Crystallization of the A-DNA structure appears to require an additional loss in water activity that would result from the longer equilibrium time during crystal growth. This supports our contention that E-DNA is more hydrated than A-DNA in this sequence.

## Solvent interactions in E-DNA

The deep major groove and shallow minor groove, along with the relatively noninclined base pairs result in a more exposed surface for E-DNA. The solvent accessible surface area of a base pair in E-DNA (288 Å$^2$) is >3 Å$^2$ more exposed than in A-DNA (285 Å$^2$) or B-DNA (284 Å$^2$). A well-defined set of water molecules is observed in the major groove of E-DNA, all hydrogen bonded to, and in the plane of, the base pairs. However, the large rise and slide between base pairs keep these waters from forming a regular spine. Instead, the waters in E-DNA sit on the exposed face of the adjacent stacked base pair (Fig. 3*a*). The solvent structure in the minor groove is obscured by the symmetry related duplex that sits against this groove.

E-DNA provides a structural rationale for the higher rate of spontaneous deamination in methylated cytosines (Fig. 3*b*), which leads to the transition mutation of $dm^5C$-dG to dT-dA base pairs. The rate of this mutation is 21-fold higher when the cytosine bases in duplex DNAs are methylated[18]. We compared the structure of the central d(CpG) step and the associated waters of $d(GGCGCC)_2$ as B-DNA and $d(GGCGm^5CC)_2$ and $d(GGCGBr^5CC)_2$ as E-DNA to illustrate how conformation rather than specific methylation would facilitate the deamination reaction. The CpG step of each structure has a water molecule hydrogen bonded to the basic N7 nitrogen and lying in the plane of the guanine base. The waters in the B-DNA dinucleotides are located 4.5 Å to >6 Å from the edges of the stacked cytosines (Fig. 3*a*). However, the shifted base pairs in E-DNA position the solvent molecules just above and within 3.8–4.2 Å of the exposed C4 carbon of the pyrimidine base. In addition, these waters in E-DNA are nearly perpendicular to the cytosine base plane, a geometry that would facilitate nucleophilic attack of the aromatic ring. When the cytosine of the d(CpG) step in E-DNA is modeled as the hemiaminal intermediate of the deamination reaction, the resulting hydroxyl oxygen is 2.0–3.0 Å from the N7 nitrogen and in the plane of the guanine base (Fig. 3*c*). The CpG dinucleotide in this E-DNA model, therefore, can potentially stabilize the hemiaminal intermediate through hydrogen bonds.

**Table 1 Average helical parameters[1] for hexanucleotides containing dC-dG, $dm^5C$-dG, and $dBr^2C$-dG base pairs as A-DNA[2], B-DNA, and E-DNA**

| Parameter | A-DNA[2] | B-DNA | E-DNA | |
|---|---|---|---|---|
| Helical twist (°) | 31.5 ± 3.6 | 34.8 ± 3.5 | 29.2 ± 4.5 | (30.6 ± 3.5) |
| Rise (z-displacement) (Å) | 2.8 ± 0.32 | 3.30 ± 0.28 | 3.56 ± 0.36 | (3.71 ± 0.19) |
| Slide (Å) | -1.99 ± 0.27 | -0.63 ± 0.57 | -2.32 ± 0.17 | (-2.39 ± 0.13) |
| Roll angle (°) | 9.0 ± 4.7 | 2.9 ± 4.0 | 2.1 ± 4.4 | (0.9 ± 4.0) |
| x-Displacement (Å) | -4.73 ± 0.37 | -1.60 ± 0.75 | -3.38 ± 0.51 | (-3.43 ± 0.55) |
| Inclination angle (°) | 15.2 ± 4.3 | 7.4 ± 5.7 | -4.6 ± 4.1 | (-6.1 ± 1.9) |

[1]Mean values are shown ±1 standard deviation. Values in parentheses were calculated for E-DNA in the absence of the stacked terminal base pairs.
[2]From ref. 5.

**Table 2 Data collection and refinement statistics**

| | $d(GGCGCC)_2$ + $Co(NH_3)_6^{3+}$ | $d(GGCGCC)_2$ + $Spermine^{4+}$ | $d(GGCGm^5CC)_2$ E-DNA | $d(GGCGBr^5CC)_2$ E-DNA | $d(GGCGm^5CC)_2$ A-DNA |
|---|---|---|---|---|---|
| **Data collection**[1] | | | | | |
| Space group | $P4_122$ | $P4_12_12$ | $P4_32_12$ | $P4_32_12$ | $C222_1$ |
| Unit cell lengths (Å) | a = b = 42.6, c = 63.3 | a = b = 71.5, c = 59.6 | a = b = 62.1, c = 24.3 | a = b = 60.4, c = 24.7 | a = 37.1, b = 46.8, c = 110.7 |
| Resolution (Å) | 42.59–2.6 | 71.5–2.7 | 20.0–2.2 | 60.4–2.25 | 20.0–2.0 |
| Total reflections (unique) | 20,150 (2,026) | 32,859 (4,551) | 23,113 (2,571) | 31,302 (2,393) | 27,952 (6,053) |
| Completeness (%)[2] | 99.9 (99.9) | 98.8 (96.6) | 95.7 (91.6) | 99.9 (99.9) | 88.6 (62.9) |
| $R_{merge}$ (%)[2,3] | 6.1 (25.1) | 5.7 (39.5) | 4.9 (51.3) | 5.0 (34.7) | 5.5 (38.4) |
| **Refinement** | | | | | |
| Resolution (Å) | 8.0–2.6 | 8.0–2.7 | 8.0–2.2 | 8.0–2.25 | 8.0–2.0 |
| $R_{cryst}$ ($R_{free}$) (%)[4] | 20.5 (27.9) | 22.6 (28.8) | 21.0 (27.3) | 19.3 (25.6) | 20.5 (24.8) |
| DNA (solvent) atoms | 240 (22) | 600 (37) | 242 (29) | 242 (28) | 693 (126) |
| R.m.s. deviations | | | | | |
| Bond lengths (Å) | 0.005 | 0.006 | 0.007 | 0.004 | 0.003 |
| Bond angles (°) | 1.095 | 0.981 | 0.903 | 0.674 | 0.811 |

[1]X-ray diffraction data were collected at room temperature using CuKα radiation from a Rigaku RUH3R generator and an R-AXIS IV image plate detector, and reduced using the programs Denzo and Scalepack from the HKL package[26] and D*Trek[27].
[2]Values in parentheses refer to the highest resolution shell.
[3]$R_{merge} = \Sigma_{hkl}\Sigma_i|I_{hkl,i} - \langle I\rangle_{hkl}| / \Sigma_{hkl}\Sigma_i|I_{hkl,i}|$ where $I_{hkl}$ is the intensity of a reflection and $\langle I\rangle_{hkl}$ is the average of all observations of this reflection and its symmetry equivalents.
[4]The B-DNA and E-DNA structures were refined with the program X-PLOR 3.851 (ref. 19), incorporating nucleic acid specific parameters[28]. The A-DNA structure of $d(GGCGm^5CC)_2$ was refined using CNS[29]. $R_{cryst} = \Sigma_{hkl}|F_o - kF_c| / \Sigma_{hkl}|F_o|$. $R_{free} = R_{cryst}$ with 10% of the reflections that were not used in refinement[30].

## Methods

**Crystallization and structure determination.** The sequence $d(GGCGCC)_2$ was crystallized from solutions containing 0.7 mM DNA, 25 mM sodium cacodylate buffer (pH 6), 0.8 mM $MgCl_2$, and 0.75 mM spermine tetrahydrochloride equilibrated against a reservoir of 15% (v/v) 2-methyl-2,4-pentanediol (MPD) and from this same solution with 1–2 mM $Co(NH_3)_6^{3+}$ added. The cobalt form (Table 2) was solved using two separate B-DNA d(GGC/GCC) duplexes in a directed real space translation/rotation/rigid body search (X-PLOR 3.851 (ref. 19) script written in this lab). The refined structure was then used to solve the structures of three stacked B-DNA duplexes in the spermine crystal form. The solvent content of the spermine form is ~70% greater than typical B-DNA crystals[20], and could not be accurately modeled in the structure. This explains the moderate resolution and relatively high R-values of this structure.

The sequences $d(GGCGm^5CC)_2$ and $d(GGCGBr^5CC)_2$ were crystallized from solutions containing 0.7 mM DNA, 25 mM sodium cacodylate (pH 6), 0.8 mM $MgCl_2$, and 0.1–0.5 mM spermine tetrahydrochloride equilibrated against a reservoir of 15–20% (v/v) MPD. The structure of the brominated sequence was solved first by molecular replacement with the program AMoRe[21], using the central four base pairs of an ideal A-DNA structure as the search model. This was subsequently subjected to simulated annealing, followed by hand fitting of the terminal base pairs to the residual electron density observed in an $F_o - F_c$ difference map. The refined brominated model was used as a search model to solve the structure of the methylated sequence.

A-DNA crystals of $d(GGCGm^5CC)_2$ that grew after two to three months from the same set of crystallization solutions and identical conditions that yielded E-DNA crystals were solved by molecular replacement using the A-DNA structure of $d(GCCGGC)_2$[5] in the program AMoRe[21].

**Coordinates.** Coordinates have been deposited in the Protein Data Bank (accession codes: 1F6C for the spermine$^{4+}$ and 1F69 for the $Co(NH_3)_6^{3+}$ forms of $d(GGCGCC)_2$ as B-DNA; 1F6I for $d(GGCGm^5CC)_2$ and 1F6J for $d(GGCGBr^5CC)_2$ as E-DNA; and 1F6E for $d(GGCGm^5CC)_2$ as A-DNA).

**Acknowledgments**

We thank B.H.M. Mooers and the P.A. Karplus laboratory for helpful discussion, and K.E. van Holde, C.K. Mathews, and W.C. Johnson, Jr. for reading this manuscript. This work was supported by the National Science Foundation, the Oregon American Cancer Society, and the Environmental Heath Science Center at OSU. X-ray facilities were funded in part by the M.J. Murdock Charitable Trust.

Correspondence should be addressed to P.S.H. *email: hops@ucs.orst.edu*

Received 2 March, 2000; accepted14 June, 2000.

1. Noyer-Weidner, M. & Trautner, T.A. In *DNA methylation: molecular biology and biological significance.* (eds, Jost, J.P. & Saluz, H.P.), 39–108 (Birkhäuser Verlag, Boston; 1993).
2. Singer-Sam, J. & Riggs, A.D. In *DNA methylation: molecular biology and biological significance.* (eds, Jost, J.P. & Saluz, H.P.) 358–384 (Birkhäuser Verlag, Boston; 1993).
3. Sasaki, H., Allen, N.D. & Surani, M.A. In *DNA Methylation: Molecular Biology and Biological Significance.* (eds Jost, J.P. & Saluz, H.P.) 469–486 (Birkhäuser Verlag, Boston, 1993).
4. Antequera, F. & Bird, A. In *DNA methylation: molecular biology and biological significance.* (eds, Jost, J.P. & Saluz, H.P.), 169–185 (Birkhäuser Verlag, Boston; 1993).
5. Mooers, B.H.M., Schroth, G.P., Baxter, W.W. & Ho, P.S. *J. Mol. Biol.* **249**, 772–784 (1995).
6. Frederick, C.A. *et al. Biopolymers* **26**, S145–S160 (1987).
7. Behe, M. & Felsenfeld, G. *Proc. Natl Acad. Sci. USA* **78**, 1619–1623 (1981).
8. Fujii, S., Wang, A.H.-J., van der Marel, G., van Boom, J.H. & Rich, A. *Nucleic Acids Res.* **10**, 7879–7892 (1982).
9. Timsit, Y. & Moras, D. *Methods Enzymol.* **211**, 409–429 (1992).
10. Xu, Q., Shoemaker, R.K. & Braunlin, W.H. *Biophys. J.* **65**, 1039–1049 (1993).
11. Takahara, P.M., Rosenzweig, A.C., Frederick, C.A. & Lippard, S.J. *Nature* **377**, 649–652 (1995).
12. Arnott, S., Chandrasekaran, R., Millane, R.P. & Park, H.-S. *J. Mol. Biol.* **188**, 631–640 (1986).
13. Doucet, J., Benoit, J.-P., Cruse, W.B.T., Prange, T. & Kennard, O. *Nature* **337**, 190–192 (1989).
14. Mayer-Jung, C., Moras, D. & Timsit, Y. *EMBO J.* **17**, 2709–2718 (1998).
15. Timsit, Y. & Moras, D. *EMBO J.* **13**, 2737–2746 (1994).
16. Wang, A.H.-J., Fujii, S., van Boom, J.H. and Rich, A. *Proc. Natl. Acad. Sci. USA* **79**, 3968–3972 (1982).
17. Ng, H.-L., Kopka, M.L., & Dickerson, R.E. *Proc. Natl. Acad. Sci. USA* **97**, 2035–2039 (2000).
18. Zhang, X. & Mathews, C.K. *J. Biol. Chem.* **269**, 7066–7069 (1994).
19. Brünger, A.T. *X-PLOR version 3.1: a system for X-ray crystallography and NMR*. (Yale University Press, New Haven, Connecticut; 1992).
20. Dickerson, R.E. *Methods Enzymol.* **211**, 67–111 (1992).
21. Navaza, J. *Acta Crystallogr. A* **50**, 157–163 (1994).
22. Lavery, R. & Sklenar, H. *J. Biomol. Struct. Dyn.* **6**, 655–667 (1989).
23. Merritt, E.A. & Bacon, D.J. *Methods Enzymol.* **277**, 505–524 (1997).
24. Carter, C.W., Jr. *Biochimie* **77**, 92–98 (1995).
25. Weiner, S.J. *et al. J. Am. Chem. Soc.* **106**, 765–784 (1984).
26. Otwinowski, Z. & Minor, W. *Methods Enzymol.* **276**, 307–326 (1997).
27. Pflugrath, J.W. *Acta Crystallogr. D* **55**, 1718–1725 (1999).
28. Parkinson, G., Vojtechovsky, J., Clowney, L., Brünger, A.T. & Berman, H.M. *Acta Crystallogr. D* **52**, 57–64 (1996).
29. Brünger, A.T. *et al. Acta Crystallogr. D* **54**, 905–921 (1998).
30. Brünger, A.T. Nature **355**, 472–475 (1992).